Analysis of the subcellular targeting of the smaller replicase protein of *Pelargonium flower break virus*

Sandra Martínez-Turiño, Carmen Hernández*

Instituto de Biología Molecular y Celular de Plantas (CSIC-Universidad Politécnica de Valencia). Ciudad Politécnica de la Innovación, Ed. 8E. Camino de Vera s/n, 46022 Valencia, Spain

* Corresponding author. Mailing address: Carmen Hernández, Instituto de Biología Molecular y Celular de Plantas, (CSIC-Universidad Politécnica de Valencia). Ciudad Politécnica de la Innovación, Ed. 8E. Camino de Vera s/n, 46022 Valencia, Spain

Phone: 34-96-3877869 Fax: 34-96-3877859 E-mail: cahernan@ibmcp.upv.es

ABSTRACT

Replication of all positive RNA viruses occurs in association with intracellular membranes. In many cases, the mechanism of membrane targeting is unknown and there appears to be no correlation between virus phylogeny and the membrane systems recruited for replication. *Pelargonium flower break virus* (PFBV, genus *Carmovirus*, family *Tombusviridae*) encodes two proteins, p27 and its readthrough product p86 (the viral RNA dependent-RNA polymerase), that are essential for replication. Recent reports with other members of the family *Tombusviridae* have shown that the smaller replicase protein is targeted to specific intracellular membranes and it is assumed to determine the subcellular localization of the replication complex. Using *in vivo* expression of green fluorescent protein (GFP) fusions in plant and yeast cells, we show here that PFBV p27 localizes in mitochondria. The same localization pattern was found for p86 that contains the p27 sequence at its N-terminus. Cellular fractionation of p27GFP-expressing cells confirmed the confocal microscopy observations and biochemical treatments suggested a tight association of the protein to membranes. Analysis of deletion mutants allowed identification of two regions required for targeting of p27 to mitochondria. These regions mapped toward the N- and C-terminus of the protein, respectively, and could function independently though with distinct efficiency. In an attempt to search for putative cellular factors involved in p27 localization, the subcellular distribution of the protein was checked in a selected series of knockout yeast strains and the outcome of this approach is discussed.

Keywords. Carmovirus; *Pelargonium flower break virus*; viral replicase, subcellular localization; mitochondria; membrane association

1. Introduction

The replication of all positive strand RNA viruses of eukaryotes takes place in membrane-associated complexes in the cytoplasm of infected cells. The reasons for membrane association of viral RNA synthesis are not well understood. It is generally believed that the membranes play a structural and/or organizational role during assembly of the replication machinery and permit to increase the local concentration of replicative enzymes and viral RNAs. In addition, the compartmentalization of the replication process may prevent double-stranded viral replication intermediates from being sensed by antiviral defence systems of the host cell (Denison, 2008; Mackenzie, 2005). Membrane systems that can be compromised in viral replication include plasma membrane, endoplasmic reticulum, Golgi apparatus, vacuoles, chloroplasts, mitochondria, peroxisomes and endo/lysosomes (reviewed in Ahlquist et al., 2003; Salonen et al., 2005). In many cases the replication complexes also induce morphological alterations of the target membranes, which can interfere with their normal functions.

Pelargonium flower break virus is a member of the genus *Carmovirus* in the family *Tombusviridae*. Its genome consists of a monopartite, positive-sense RNA of 3,923 nt which is neither capped nor polyadenylated and contains five open reading-frames (ORFs) (Rico and Hernández, 2004). Proteins encoded by the internal and 3´-terminal ORFs are dispensable for PFBV multiplication and are rather involved in viral movement, encapsidation or suppression of RNA silencing (Martínez-Turiño and Hernández, 2009; 2011). In contrast, the translation products of the ORFs located 5´-proximal in the genomic RNA, ORFs 1 and 2, correspond to polypeptides of 27 and 86 kDa, respectively, that are strictly required for viral replication (Martínez-Turiño and

63 Hernández, 2010). The larger replicase protein (p86) is synthesized as a readthrough
64 product of the shorter one (p27) and, due to the low frequency of the stop codon
65 suppression even, the latter is synthesized at 10-20 fold higher amounts than the former
66 (Fernández-Miragall and Hernández, 2011). While p86 encloses the eight motifs
67 conserved in the viral RNA dependent-RNA polymerases (RdRp) of supergroup II of
68 the positive strand RNA viruses (Koonin, 1991; Koonin and Dolja, 1993), p27 has no
69 obvious replication motifs as occurs with equivalent proteins in the family
70 *Tombusviridae*.

71 The specific role of the smaller replicase protein of members of the family
72 *Tombusviridae* has long been a subject of debate. Recent results with PFBV p27 and
73 previous ones with the homologous product of *Tomato bushy stunt virus* (TBSV),
74 namely p33, have revealed that these proteins bind cognate viral ssRNAs with high
75 affinity suggesting that play an essential role in selection and recruitment of replication
76 templates (Martínez-Turiño and Hernández, 2010; Pogany et al., 2005; Rajendran and
77 Nagy, 2003). Other roles, however, cannot be discarded. Indeed, a recent report
78 indicates that TBSV p33 has RNA chaperone activity and likely facilitates proper
79 folding of viral RNAs during replication (Stork et al., 2011). In addition, in the last
80 years distinct studies with species of the genera *Tombusvirus, Dianthovirus* and
81 *Panicovirus* have shown that the protein encoded by ORF1 is targeted to specific
82 intracellular membranes and it is assumed to determine the subcellular localization of
83 the replication complex. The specific membrane system recruited varies from one virus
84 to another. Thus, the ORF1 products of *Red clover necrotic mosaic virus* (RCNMV,
85 genus *Dianthovirus)* and of *Panicum mosaic virus* (PMV, genus *Panicovirus*) associate
86 to membranes of the endoplasmic reticulum (Batten et al., 2006; Turner et al., 2004),
87 whereas the ORF1 products of TBSV, *Cymbidium ringspot virus* (CymRSV) and

Cucumber necrosis virus (CNV) in the genus *Tombusvirus,* are targeted to peroxisomes (McCartney et al., 2005; Navarro et al., 2004; Panavas et al., 2005). Despite *Carnatian italian ringspot virus* (CIRV) belongs also to genus *Tombusvirus,* its ORF1 product (p36) is sorted to mitochondria (Weber-Lotfi et al., 2002). Most of these proteins induce organelle aggregation and/or proliferation of the membranes they associate with and seem to be truly integrated in the corresponding membranes. In many cases, α-helices that function as transmembrane domains (TMs) play a critical role in both targeting and integration to specific membranes. That is the case of CIRV p36 that has been proposed to associate to the mitochondrial outer membrane through two TMs and multiple recognition signals present at the N-terminus that might function cooperatively as a so-called signal loop-anchor type mitochondrial targeting sequence (Weber-Lotfi et al., 2002; Hwuang et al., 2008).

Information on the membrane association of replication proteins from members of the genus *Carmovirus* is relatively scarce. Recently, the interaction of the ORF1 product (p29) of *Melon necrotic spot virus* (MNSV) with mitochondrial membranes has been described and at least one TM has been found to be required for such interaction (Mochizuki et al., 2009). In addition, the presence of N-terminal, classical mitochondrial targeting signals (MTS), that consist of 15 to 40 amino acid (aa) residues and form positively charged amphipathic α-helices (Chacinska et al., 2009), was suggested for the ORF1 products of other carmoviruses (Ciuffreda et al., 1998) but experimental approaches to study the subcellular sorting of other carmoviral replicase proteins have not yet been made.

Here we show that PFBV p27 is able to target the green fluorescent protein (GFP) reporter to mitochondria *in vivo* upon transient expression of a fusion protein in plant and yeast cells. Similar results were obtained with the complete replicase p86 which

contains the p27 sequence at its N-terminal region. Analysis of deletion mutants indicated that two regions toward the N- and C-terminus, respectively, of p27 contain signals for mitochondrial targeting. Biochemical fractionation experiments revealed that p27 sedimented mainly with mitochondrial enriched fractions, in agreement with the confocal microscopy observations, and that associates tightly to membranes. Finally, the subcellular distribution of the protein was checked in a selected series of knockout yeast strains in an attempt to search for putative cellular factors involved in p27 localization.

2. Materials and methods

2.1. Generation of constructs

For protein expression in *Saccharomyces cerevisiae*, the GFP gene was cut out from pBin19-s*gfp* (Peña et al., 2003) with *Bam*HI/*Eco*RI digestion and subcloned into the *Bam*HI/*Eco*RI sites of plasmid pYES 2.0 (Invitrogen) containing the galactose-activated GAL1 promoter. The resulting recombinant plasmid was named pYES-GFP. In addition, the PFBV p27 coding sequence was amplified with Expand High Fidelity PCR System (Roche) using the PFBV infectious clone pSP18-IC (Rico and Hernández, 2006) as template, and primers CH67 and CH70 which harboured an *Nco*I restriction site at their 5´ end (primers listed in Supplemnetary Table 1). After *Nco*I digestion, the PCR-generated fragment was cloned in the *Nco*I site which precedes the start codon of the GFP gene in construct pYES-GFP to yield pYES-p27GFP that contained the p27 cDNA fused in frame to the GFP gene. A similar construct, signed as pYES-p86GFP, was prepared with the p86 gene which was PCR amplified with primers CH67 and CH182 (Supplementary Table 1) from plasmid p27tyr, a full-length PFBV clone in which the amber stop codon of ORF1 was mutated to a tyrosine codon (Martínez-

Turiño and Hernández, 2010). To study possible co-localization of p27 and p86, the GFP gene of plasmid pYES-p86GFP was replaced by the gene encoding the monomeric red fluorescent protein (mRFP) yielding construct pYES-p86mRFP. The complete expression cassette of this construct (the p86mRFP fusion gene flanked by the GAL1 promoter and the terminator sequence) was PCR amplified with primers CH222 and CH223, encompassing a *Spe*I restriction site at their 5´ end (Supplemnetary Table 1), subsequently digested with *Spe*I and ligated into plasmid pYES-p27GFP through the *Spe*I site present in the vector sequence. The resulting construct with two expression cassettes in tandem was named pYES-p27GFP/p86mRFP.

Different regions of the p27 gene were also PCR amplified with specific primers (Table 1) and fused in frame with the GFP gene of construct pYES-GFP using appropriate restriction sites (introduced by PCR into the p27 derived cDNAs). Following this approach, a total of thirteen p27 deletion mutant constructs were generated: pYES-p27(21-243)GFP (mutant 1, created with primers CH115 and CH70), pYES-p27(34-243)GFP (mutant 2, primers CH113/CH70), pYES-p27(73-243)GFP (mutant 3, primers CH162/CH70), pYES-p27(1-215)GFP (mutant 4, primers CH67/CH114), pYES-p27(1-180)GFP (mutant 5, primers CH150/CH215), pYES-p27(1-162)GFP (mutant 6, primers CH150/CH228), pYES-p27(1-155)GFP (mutant 7, primers CH150/CH163), pYES-p27(21-155)GFP (mutant 8, primers CH115/CH163), pYES-p27(73-155)GFP (mutant 9, primers CH162/CH163), pYES-p27(51-155)GFP (mutant 10, primers CH318/CH163), pYES-p27(34-155)GFP (mutant 11, primers CH113/CH163), pYES-p27(73-162)GFP (mutant 12, primers CH162/CH228), and pYES-p27(73-215)GFP (mutant 13, primers CH162/CH114).

For transient expression of proteins in *Nicotiana benthamiana* protoplasts, the GFP gene, the cDNA encoding the p27GFP fusion and GFP fusions with the p27 derivatives

of mutants 3, 8, 10, and 13 were recovered from the corresponding yeast constructs with *Bam*HI/*Pst*I digestion and subcloned into the *Bam*HI/*Pst*I sites of a pBluescript KS+ derived-plasmid containing the *Cauliflower mosaic virus* (CaMV) 35S promoter upstream of the *Bam*HI site and the terminator sequence of the *Solanum tuberosum* proteinase inhibitor II gene downstream of the *Pst*I site. All constructs were routinely sequenced to avoid unwanted modifications.

2.2. Expression of gene constructs in yeast and plant cells

For expression in yeast cells, the pYES 2.0 derived constructs were employed to transform *S. cerevisiae* strain W303-1A (*MATα, his3-11/15*, *leu2-3/112*, *trp1-1*, *ura3-1*, *ade2-1*, *can1-100,* Wallis et al., 1989). The plasmid p36K-GFP, allowing expression of protein p36 of *Carnation italian ringspot virus* (Rubino et al., 2000), was also included for comparison purposes. Transformation of plasmids was done with the lithium acetate-polyethylene glycol method (Ito et al., 1983). Transformed cells were spread on minimal selective medium (SD) plates containing 0.7 % yeast nitrogen base without amino acids, 2 % dextrose or galactose, histidine at 30 μg/ml, leucine at 100 μg/ml, tryptophan at 100 μg/ml and 2 % agar, and incubated at 28 ºC for two days. Samples were collected directly from the plates for inspection through confocal microscopy. To study potential involvement of host factors in p27 subcellular localization, a series of yeast knockout strains (see Table I) coming from the EUROSCARF collection (Winzeler et al., 1999) was also transformed with construct pYES-p27GFP. In this case, the parental, wt strain corresponded to BY4741 (*MATa; his3Δ1; leu2Δ0; met15Δ0; ura3Δ0*) and transformed cells were grown on SD/galactose plates supplemented with histidine at 30 μg/ml, leucine at 100 μg/ml, and methionine at 100 μg/ml.

For transient expression in plant cells, *N. benthamiana* protoplasts were prepared. To this aim, *N. benthamiana* leaves were incubated at 25 ºC for 3 h with 1.5 % cellulose and 0.4 % macerozyme (both enzymes from Duchefa Biochemie) in 0.6 M mannitol. The protoplasts were then filtered through a nylon membrane (35-75 μm), collected through 1 min centrifugation at 100 x *g*, washed twice with solution W5 (154 mM NaCl, 125 nM $CaCl_2$, 5 mM KCl and 2 mM HEPES, pH 5.7) and incubated for 30 min on ice. For plasmid delivery, the protoplasts were adjusted to 10^6/ml in a medium containing 0.4 M mannitol, 15 mM $MgCl_2$ and 4 mM MES (pH 5.7). About 20 μg of the corresponding plasmid was added to 10^5 protoplasts in a medium containing 0.1 M mannitol, 20 % PEG 4000 and $CaCl_2$ 50 mM. After 1 min incubation, 0.4 ml of solution W5 was added. The protoplasts were recovered by 1 min centrifugation at 100 x *g*, resuspended in 1 ml of solution W5 and incubated at 25 ºC during 24 h with continuous light. Samples were then taken for fluorescence visualization.

Mitochondria were visualized in living cells with the mitochondrial specific MitoTracker Orange CMTMRos. Staining of cells with this dye was performed following manufacturer´s recommendations (Molecular Probes). Briefly, pelleted cells were gently resuspended in a medium containing the dye at working concentration of 100 nM. Protoplasts were incubated at 25 °C for 15 min in W5 solution containing the dye. Similarly, a suspension of yeast cells in SD medium was incubated with the MitoTracker at 28 °C in orbital shaker for 30 min.

2.3. Fluorescence monitoring

Fluorescence images were obtained with a Leica TCS SL confocal laser scanning microscope employing an HCX PL APO ×40/1.25-0.75 oil CS objective. GFP derived fluorescence was monitored by excitation with a 488-nm argon laser line and emission

was visualized with a 30 nm-width band-pass window centered at 515 nm. The mRFP derived fluorescence was checked by excitation with a 543 nm green-neon laser line and fluorescence emission was collected at 610-630 nm. The MitoTracker Orange CMTMRos fluorescence was checked by excitation with a 543 nm green-neon laser line with emission being gathered at 574-584 nm.

2.4. Protein extraction and Western blot analysis

A mitochondria-enriched fraction was obtained following essentially the protocol reported by Nakai et al. (1995). Briefly, yeast cells expressing GFP or p27GFP were grown to mid-logarithmic phase in a final volume of 20 ml and collected by centrifugation. After two washings with TSB (10 mM Tris-HCl [pH 7.5], 0.6 M sorbitol), the cells were resuspended in 0.5 ml of the same buffer supplemented with 1 mM phenylmethylsulfonyl fluoride (PMSF) and, after adding 1 ml of glass beads (diameter of 0.45 to 0.5 mm), the cells were disrupted with the aid of a Mini BeadBeater programmed at maximum speed for 1 min five times with intervals of cooling on ice. Disrupted cell suspension was recovered with a pipette, avoiding contamination of glass beads, and centrifuged at 3,500 x *g* for 5 min. The supernatant was centrifuged at 12,000 x *g* for 10 min. The pellet was carefully resuspended in TSB supplemented with 1 mM PMSF and recentrifuged at 3,500 x *g* for 5 min. The resulting supernatant was centrifuged at 12,000 x *g* for 10 min, and the final pellet was washed twice with TSB and resuspended in TSB supplemented with 1 mM PMSF. Aliquots of this mitochondria-enriched fraction and its accompanying supernatant were electrophoresed, transferred to polyvinylidene difluoride (PVDF) membranes (Roche) and immunoblotted with anti-GFP (Roche). Immunoreactive bands were revealed with chemiluminescence ECL Plus kit following supplier recommendations (GE Healthcare).

In some experiments, the mitochondria-enriched fraction was incubated for 30 min on ice in the presence of one of the following reagents: 100 mM Na_2CO_3 (pH 11.3), 4 M urea or 1 M KCl. After centrifugation at 30,000 *g* for 30 min at 4°C, the pellet and supernatant were subjected to immunoblot analysis for GFP detection as indicated above.

2.5. In silico sequence analysis

Tools for protein subcellular localization prediction included CELLO v.2.5 (Yu et al., 2006), SubLoc v.1.0 (Hua and Sun, 2001), Euk-mPLoc v.2.0 (Kuo-Chen and Hong-Bin, 2010). The presence and location of potential signal peptide cleavage sites in amino acid sequence were predicted with TargetP v.1.1 (Emanuelsson et al., 2000), SignalP v.3.0 (Bendtsen et al., 2004), Protein Prowler Predictor v.1.2 (Hawkins and Bodén, 2006) and Phobius (Käll et al., 2007). Predictions of membrane-spanning regions were made with PHDhtm (Rost, 1996), TMpred (Hofmann and Stoffel, 1993), DAS (Cserzö, et al., 1997), Split v.4.0 (Juretić et al., 2002), RHYTM (Rose et al., 2009), SVMtm v.3.0 (Yuan et al., 2004), OCTOPUS (Viklund and Elofsson 2008) and ConPredII (Arai et al., 2004). An algorithm (HHELIX) developed by Orgel (2004) was applied for distinguishing helical sequences that are parallel to or “horizontal” at the membrane bilayer/aqueous phase interface, from helices that are membrane-embedded or located in extra-membranous domains. Helices included in the analysis were obtained with NPSA software (Combet et al., 2000), that provides a consensus secondary structure prediction, and the minimum helix size was set to four amino acids (for at least one complete turn of the α-helix).

3. Results

3.1. PFBV p27 shows mitochondrial localization in both yeast and plant cells

The study of the subcellular localization of p27 was firstly tackled in *S. cerevisiae*, a model system extensively used for structural and functional analysis of heterologous proteins (Galao et al., 2007; Siggers and Lesser, 2008). To this aim, the p27 coding sequence was fused in frame with the GFP gene and cloned in the yeast vector pYES 2.0 under control of the galactose-activated GAL1 promoter. A recombinant plasmid allowing expression of free GFP was also generated. Yeast cells transformed with the control GFP construct and grown on galactose-containing medium demonstrated diffuse green fluorescence throughout the cell (Fig. 1). This is due to the lack of targeting signals in GFP and its small size, which permits diffusion across the nuclear envelope. Conversely, p27 tagged with a carboxy-terminal GFP, p27GFP, localized to discrete cytoplasmic sites (Fig. 1). It was hypothesized that this cytoplasmic pattern represented localization of p27 to mitochondria, and to confirm this, the cells were stained with MitoTracker Orange, a molecular probe that specifically labels these organelle (Poot et al., 1996). It was apparent that the fluorescence derived from the p27GFP protein co-localized with the mitochondrial MitoTracker Orange signal (Fig. 1). To asses whether the larger PFBV p86 replicase protein had the same localization properties *in vivo*, the PFBV ORF2 cDNA, with the leaky stop codon of ORF1 replaced by a Tyr-encoding codon, was also fused in frame with the GFP gene and cloned into pYES 2.0 plasmid vector to allow expression of the fusion product in yeast. The p86 protein targeted GFP to organelles which were easily identified as mitochondria by their size, their shape, and the positive reaction they exhibited with the specific dye MitoTracker, yielding fluorescence images similar to those obtained previously with the p27 protein (data not

shown). This indicated that the signal(s) operating in the ORF1-derived product also operate in the context of the longer replicase protein, though the presence of additional targeting sequences in the latter one cannot be ruled out. A similar fluorescence profile was observed when p86 was fused to the monomeric red fluorescent protein (mRFP) (Fig. 1). Co-expression of p27GFP with p86mRFP in yeast cells revealed GFP- and mRFP-derived fluorescence at the same punctuate structures, indicating co-localization of the PFBV replicases (Fig. 1). In contrast with that observed for CIRV p36 (Weber-Lotfi et al., 2002 and Fig. 1), the appearance of mitochondria in yeast cells expressing PFBV p27 was indistinguishable from that of non-transformed cells (Fig. 1). Aggregation of mitochondria or membrane proliferation was neither noticed in yeast cells co-expressing p27 and p86.

To corroborate the pattern of subcellular localization of p27 in plant cells, the fusion p27GFP was cloned under the control of the 35S promoter and the resulting recombinant plasmid was used for transient expression experiments in *N. benthamiana* protoplasts. An equivalent construct allowing expression of unfused GFP was included as a control. Unfused GFP was observed through the cytoplasm and was not excluded from cell nuclei (Fig. 2). In contrast, expression of p27GFP led to a pattern of fluorescence restricted to definite structures that corresponded to mitochondria as revealed by the MitoTracker Orange signal (Fig. 2). Collectively, the results showed a clear sorting of the PFBV ORF1-encoded product to specific cell organelles, mitochondria.

3.2. PFBV p27 is tightly associated to mitochondrial membranes

The subcellular localization profiles of p27GFP indicated that it is associated with mitochondria, likely as a membrane (peripheral or integral) protein, according to that reported for other viral replicase proteins (Miller et al., 2001; Weber-Lotfi et al., 2002).

To confirm the attachment of p27 to mitochondrial membranes, a mitochondria-enriched fraction from p27GFP-expressing yeast cells was obtained. Yeast cells producing unfused GFP were used as negative control. Western blot analysis with a GFP specific antibody confirmed the presence of p27GFP in the mitochondrial fraction, in contrast with that observed for the unfused GFP that was detected in the corresponding supernatant (Fig. 3A). The mitochondrial fraction of p27GFP-expressing cells was further treated with buffers that may discriminate between peripheral and integral membrane proteins. The soluble contents were separated from the pellets by ultracentrifugation and both, pellets and supernatants, were analyzed by immunoblot with the anti-GFP sera. Most peripheral membrane proteins are dissociated from membranes by high pH, high ionic strength, or chaotropic agents**.** After treatment with 100 mM Na_2CO_3 (pH 11.3), 4 M urea or 1 M KCl, p27GFP was detected mainly in the pellets though a non-negligible amount of the protein was also found in the supernatants with the first two treatments (Fig. 3B). These observations were similar to those reported for the smaller replicase proteins of MNSV and CIRV though such polypeptides were in general more resistant to membrane extraction through biochemical treatments (Mochizuki et al., 2009; Rubino et al., 2000). We concluded from these results that p27 was membrane associated through a mechanism that imparted significant stability to protein-membrane interactions though its nature as integral membrane protein could not be confirmed.

3.3. Mapping the regions responsible for mitochondrial localization of PFBV p27

Computer analysis of p27 with a broad set of programs designed to predict protein subcellular localization on the basis of different criteria (see Material and methods section), yielded no clear results. Though some of them anticipated the observed mitochondrial sorting of the protein (e.g., CELLO v.2.5, SubLoc v.1.0, Euk-mPLoc v.2.0), the reliability of such prediction was not very high and, moreover, no clear targeting signals could be identified. The outcome of some programs (e.g., TargetP v.1.1, PProwler v.1.2, Phobius and SignalP v.3.0) pointed to the presence of a putative signal peptide toward the N-terminus of p27 that could fit the requirements of an MTS (approximately at positions 1-23) though the accuracy of such prediction was also low. This was not surprising as a large number of mitochondrial proteins, especially from the outer membrane, are not synthesized with presequences but instead contain internal targeting information of diverse nature that is difficult to predict (Chacinska et al., 2009). We also searched for potential hydrophobic α-helices that could act as TMs and function as signal-anchor sequences paralleling that proposed for CIRV p36 or MNSV p29 (Mochizuki et al., 2009; Weber-Lotfi et al., 2002; Hwang et al., 2008). Distinct programs (PHDhtm, TMpred, DAS, Phobius, Split v.4.0, RHYTM, SVMtm, OCTOPUS, ConPredII) predicted with moderate probability that residues 8 to 28 contained a stretch of amino acids with sufficient hydrophobicity and length to span a lipid bilayer. No other protein regions were highlighted with this approach.

As recognition of potential targeting signals in p27 through *in silico* methods was ambiguous, an initial set of seven deletion mutants was generated to evaluate the relative contributions of the different regions to mitochondrial localization. The corresponding cDNAs were fused in frame with the GFP reporter gene and placed under the control of the GAL1 promoter to study the subcellular distribution of the mutant

proteins in yeast cells. These p27 derivatives carried truncations of different extents at the N- and/or C-terminus (Fig. 4). Confocal microscopy observations showed that removal of aa up to residue 34 did not affect the mitochondrial localization of the protein despite the putative TM predicted at the N-terminus of p27 was entirely eliminated with the larger deletion (mutants 1 and 2; Fig. 4). The localization pattern was maintained when a further deletion till residue 73 was made though in this case some segregation of the fluorescence among mitochondria, cytoplasm and nucleus was observed (mutant 3; Fig. 4).

On the other side, yeast cells expressing proteins harbouring deletions at the C-terminus up to residue 155 showed GFP confined to mitochondria, giving rise to targeting pictures that were essentially identical to those obtained with the wt p27 (mutants 4 to 7; Fig. 4). At this point, the results suggested the presence of either a targeting signal among residues 73-155 (common to all constructs) or two independent signals located toward the N- and C-termini of the protein. To discriminate between these two possibilities, another set of six mutants was analyzed (mutants 8 to 13; Fig. 5). A truncated protein retaining residues 21 to 155 showed the typical mitochondrial pattern (mutant 8; Fig. 5). However, an additional deletion at the N-terminus till residue 73 led to loss of the mitochondrial targeting with the fluorescence being distributed through in the cytosol and nucleus as observed in cells expressing unfused GFP (mutant 9; Fig. 5). These observations argued against the existence of a targeting signal among residues 73 and 155 and supported instead the presence of a relevant sequence at the N-terminus between residues 21 to 73. In order to map more precisely such signal sequence, a couple of intermediate deletions were performed. The fluorescence of a truncated protein harbouring residues 51 to 155 was observed in the cytoplasm and nucleus whereas another truncated protein encompassing residues 34-155 showed the

fluorescence associated to mitochondria though part of it was also detected through the cytosol and nucleus (mutants 10 and 11, respectively; Fig. 5). These results suggested that the region responsible for mitochondrial targeting was incomplete in the last construct and confine such region to residues 21-50.

Comparison of the localization patterns of mutants 3 (Fig. 4) and 9 (Fig. 5) together with the above results, hinted at the presence of another targeting signal among residues 155-243. Two additional truncated variants, mutants 12 and 13 (Fig. 5), were analyzed and the associated fluorescence was found to be scattered through cytoplasm and nucleus. As fluorescence of mutant 3 was observed to some extent, though not exclusively, associated to mitochondria, we can concluded that another sorting signal, presumably weaker than that found to the N-terminus, is present between residues 215-243.

To corroborate that the regions found to be responsible for targeting of p27 to mitochondria in yeast were also operative in plant cells, cDNAs of a set of informative p27 derivatives tagged with a carboxy-terminal GFP were cloned under the control of the 35S promoter and expressed in *N. benthamiana* protoplasts. As observed in yeast, fluorescence derived from mutant 10, encompassing residues 51-155, was uniformly distributed through the cytoplasm and nucleus but enlargement at the N-terminus up to residue 21 in mutant 8, resulted in fluorescence restricted to defined structures that were identified as mitochondria by staining with the MitoTracker dye (Fig. 6). These observations confirmed the role of the region encompassing residues 21-50 in mitochondrial targeting. In addition, the pattern of fluorescence derived from mutant 13 was essentially identical to that of the unfused GFP whereas that of mutant 3 was found associated, at least partially, to mitochondria (Fig. 6). Thus, the results obtained in

protoplasts paralleled those obtained in yeast and pointed to the presence of a targeting signal toward the N-terminus of p27 and another, weaker signal toward the C-terminus.

3.4. The mitochondrial localization of PFBV p27 in yeast is not affected in a selected series of knockout yeast strains

In order to approach the potential involvement of cellular factors in correct targeting of p27, the pattern of subcellular localization of the PFBV replicase protein was analyzed in yeast strains lacking some representative proteins either of the outer mitochondrial membrane or of other locations with putative or proven role in mitochondrial sorting. The twenty-two mutants checked are shown in Table I and have been arranged on the basis of their functional annotations. One first group included components of the translocase outer membrane (TOM) and of the sorting and assembly machinery (SAM) (TOM70, TOM7, TOM6, TOM5, TOM72, SAM37). The TOM complex represents the general entry gate of the vast majority of mitochondrial proteins whereas the SAM complex plays a main role in insertion of β-barrel outer membrane proteins, a process in which TOM components are also involved (reviewed in Chacinska et al., 2009). Other cellular factors tested included a chaperone involved in the transfer of precursor proteins to the carrier translocase of the inner membrane as well as in directing b-barrel proteins to the outer membrane (TIM9), components of the endoplasmic reticulum-mitochondrial encounter structure (ERMES) (MDM34, MDM10, MMM1), subunits of the heteromeric nascent polypeptide-associated complex (NAC) implicated in protein sorting and translocation (EGD1, EGD2), elements of the ubiquitin pathway (SEL1, UBP16), mitochondrial porins (POR1, POR2), a membrane-spanning ATPase involved in sorting of proteins in the mitochondria (MSP1), a mitochondrial phosphate carrier (MIR1), factors that regulate mitochondrial fusion or

morphology (GEM1, UGO1), and other proteins of uncertain function but that are major components of the mitochondrial outer membrane (OM45, MMR1). Competent cells of the distinct mutant strains were prepared and transformed with the construct that allows expression of the p27GFP. Fluorescence derived from the fusion polypeptide was analyzed in each mutant by confocal microscopy. In all cases, the pattern of the subcellular localization of p27GFP was indistinguishable from that observed in the wt strain (Fig. 7 and data not shown) indicating that none of the factors whose expression was abolished has a significant role in the mitochondrial targeting of the protein.

4. Discussion

In this study, we have first investigated the intracellular localization, membrane association, and organelle-targeting signals of p27, the smaller replicase protein of PFBV. The experiments have been performed in both plant and yeast cells, as the latter represent a versatile model system that is being widely used to study specific aspects of plant/animal virus replication (Galao et al., 2007; Nagy, 2008). The results have shown a clear targeting of p27 to mitochondria, paralleling that reported for CIRV p36 and MNSV p29 which are related tombusviral and carmoviral replicases, respectively (Mochizuki et al., 2009; Rubino et al., 2001; Weber-Lotfi et al., 2002). The observation would be also consistent with the outcome of electronic microscopy studies showing that PFBV infection specifically affects mitochondria, hinting at this organelle as the sites of RNA synthesis (Lesemann and Adam, 1994).

Analysis of the subcellular localization of PFBV p86 has revealed that it also localizes in mitochondria. This was an expected result as the PFBV p86 RdRp protein includes the entire p27 sequence in its N-terminus, and thus contains the same mitochondrial targeting information. Confocal microscopy has also shown that PFBV

445 p27 and p86 co-localize in yeast (Fig. 1), suggesting that both products function
446 together to form a replication complex, likely establishing protein-protein interactions.
447 Supporting this view, interactions among the small and the large replicase proteins have
448 been reported for members of the genus *Tombusvirus* (Rajendran and Nagy, 2006) and
449 similar interactions might occur in related viruses, including PFBV.

450 As the localization pattern of p27 was not modified when co-expressed with its
451 allied replication protein p86, the study of the mitochondrial targeting information of
452 the protein when expressed on its own was esteemed appropriate. To facilitate
453 dissection of putative mitochondrial signal(s), a battery of p27-deletion mutants were
454 expressed initially in *S. cerevisiae* and its intracellular location was investigated by
455 confocal microscopy. The results obtained in the yeast system were essentially
456 reproduced in plant cells, substantiating the usefulness of the former system for
457 elucidation of structural and functional properties of heterologous proteins of eukaryotic
458 origin. The putative signal peptide predicted at the N-terminus was not needed for p27
459 localization in mitochondria, in line with the dispensability of putative MTSs at the N-
460 terminus of MNSV p29 and CIRV p36 (Mochizuki et al., 2009; Weber-Lotfi et al.,
461 2002). Instead, a predominant role of a region contained among aa residues 21 and 50
462 was highlighted and a lesser, but significant contribution of the C-terminus (residues
463 216-243) could also be ascertained. In fact, the latter region seems to be operative by
464 itself in directing the protein to mitochondria but the segregating localization pattern of
465 the derivatives containing this segment but lacking the N-terminal region (see mutant 3
466 in Fig. 4 and 6), suggests it has limited targeting potential. *In silico* analysis of the
467 protein did not revealed clear structural traits in the delineated regions. The unique TM
468 predicted at the N-terminus, among positions 8-28, was not entirely required for perfect
469 localization of the protein to mitochondria as mutant 8 (Fig. 5), with just eight residues

of the predicted TM, showed the same localization pattern as the wt protein. On the basis of this observation and of the lack of a putative TM in the C-terminal region, we considered the possibility of p27 being associated to membrane throughout surface (SM) helices, that are parallel to or "horizontal" at the membrane bilayer, rather than throughout TM helices. SM helices are difficult to characterize due to the problems in obtaining high-resolution structural data (reviewed by Orgel, 2004; 2006). They have been proposed to play an ancillary role to TM helices though they might mediate binding to membranes in the absence of membrane-spanning helices (Garavito et al., 1995; Lomize et al., 2006). We have applied a protocol developed by Orgel (2004, 2006) for distinguishing SM helical sequences from helices that are membrane-embedded or located in extra-membranous domains. Through this method, two SM helices could be predicted in p27 (Fig. 8). Remarkably, SM1 and SM2 would be enclosed, respectively, within the N- and the C-terminal stretches required for mitochondrial targeting, suggesting that they could be important for subcellular localization. Further investigation will help to establish whether this prediction fits the real situation.

In agreement with the subcellular distribution of p27 revealed by confocal microscopy, the protein co-fractionated with mitochondria isolated from transformed yeast cells. Biochemical analyses suggested a tight association of the replicase protein with membranes though it was partially displaced from mitochondrial fractions through carbonate or urea treatments. Such displacement may further support the hypothesis that the association of the protein with the membranes occurs via surface helices that might promote strong association to membranes (Garavito et al., 1995; Lomize et al., 2006) but logically weaker than that provided by truly integration throughout TMs. We cannot, however, dismiss other scenarios with the present data including interaction of

p27 with charged lipid head groups or with other membrane proteins. An example of the latter case is provided by the tobamovirus replicase proteins that are closely associated to membranes despite that they do not contain membrane-targeting signals or membrane-spanning regions, an association that seems to be mediated by interaction with a seven-pass transmembrane protein (reviewed by Ishibashi et al., 2010).

No obvious similarities can be detected among the regions that direct mitochondrial targeting of PFBV p27 and of CIRV p36 or MNSV p29. Another striking distinction concerns to the absence of noticeable membrane proliferation or mitochondrial aggregation in PFBV p27-expressing cells in contrast with that observed in cells expressing CIRV p36 or MNSV p29 (Mochizuki et al., 2009; Rubino et al., 2000). This observation was not surprising as mitochondrial membrane proliferation is absent in natural infections by PFBV and only dilation of mitochondrial cristae is observed (see Lesemann and Adam, 1994). Therefore, no proliferation of the mitochondrial outer membrane should be expected upon expression of the p27 alone. These results suggest that related small replication proteins may differ in their “modus operandi” and expands the diversity found among this type of products in the family *Tombusviridae* that, despite their moderate-to-high sequence homology, are each selectively targeted to a specific organelle. Such organelle may be dissimilar among members of the same genus (McCartney et al., 2005; Navarro et al., 2004; Panavas et al., 2005) or even among isolates of the same virus (Koenig et al., 2009).

Though no specific approaches to test it have been done, it is reasonable to assume that p27 associates with the outer membrane rather than with internal compartments of mitochondria, as proposed for other viral replicase proteins targeted to this organelle (Miller et al., 2001; Weber-Lotfi et al., 2002). This localization may allow efficient multiplication of the viral genome excluding the need for a putative transmembrane

transport of the genomic RNA to access the viral replication complex (Ciufreda et al., 1998). Signals directing proteins to the outer mitochondrial membrane may be quite diverse but most of these proteins depend on surface-exposed import receptors for membrane attachment (Chacinska et al., 2009). In addition, other cellular factors, including chaperones, may have a role in delivery of proteins to mitochondria (Beddoe and Lithgow, 2002; Chacinska et al., 2009). Assessment of the subcellular localization of GFP-tagged p27 in a selected series of knockout yeast strains has shown no noticeable effect of the suppressed genes in p27 mitochondrial targeting despite several components of the TOM or the SAM complexes (Table 1) were included. These results would be in line with those obtained by Weber-Lotfi et al. (2002) showing that insertion CIRV p36 in the outer mitochondrial membrane was independent on surface-accessible receptors. It should be noted, however, that a later study revealed, through bimolecular fluorescence complementation, an interaction of CIRV p36 with some proteins of the TOM complex (Hwang et al., 2008), and thus a potential participation of import receptors in mitochondrial localization of the CIRV replicase cannot be completely ruled out. We can neither discard that elements of the TOM/SAM machinery that were not tested in the present work play a role in p27 sorting to mitochondria. In any case, no requirement of receptors for targeting to the outer mitochondrial membrane would not be exceptional as some cellular proteins have been reported to associate to this subcompartment without the aid of any cytosolic factor or TOM component (Kemper et al., 2008; Setoguchi et al., 2006) and it has been postulated that other proteins could also follow receptor-independent routes (Chacinska et al., 2009). An important element in these alternative routes could be the unique lipid composition of the mitochondrial outer membrane which shows the lowest ergosterol content among all membranes facing the cytosol (Zinser et al., 1993).

Finally, the finding of an association between PFBV p27 and mitochondrial membranes opens the possibility that the protein could modify mitochondrial functions during infection to favour viral replication. Such hypothesis has been raised for other plus strand RNA viruses though it has not been formally tested (Schwer et al., 2004). Further work is needed to explore this issue and to fully characterize the mode by which p27 is targeted to mitochondria.

Acknowledgements

We are indebted to Luisa Rubino for plasmid p36K-GFP and to Amparo Pascual-Ahuir/Markus Proft lab, including Mar Martínez-Pastor, for advice with mitochondria fractions and yeast mutants. We also thank Dolores Arocas and Isabella Avellaneda for excellent technical assistance. This research was supported by grant BFU2006-11230 and BFU2009-11699 from the Ministerio de Educación y Ciencia (MEC, Spain) and by grants ACOM/2006/210 and ACOMP/2009/040 (Generalitat Valenciana, GV) to C. H. S. M.-T. was the recipient of a predoctoral fellowship from GV and of a predoctoral contract from MEC.

561 **References**

562 Ahlquist, P., Noueiry, A.O., Lee, W.M., Kushner, D.B., Dye, B.T., 2003. Host factors in
563 positive-strand RNA virus genome replication. J. Virol. 77, 8181-8186.

564 Arai, M., Mitsuke, H., Ikeda, M., Xia, J.X., Kikuchi, T., Satake, M., Shimizu, T., 2004.
565 ConPred II: a consensus prediction method for obtaining transmembrane topology
566 models with high reliability. Nucleic Acids Res. 32, W390-W393.

567 Batten, J.S., Turina, M., Scholthof, K.B., 2006. Panicovirus accumulation is governed
568 by two membrane-associated proteins with a newly identified conserved motif that
569 contributes to pathogenicity. Virol. J. 3, 12.

570 Beddoe, T., Lithgow, T., 2002. Delivery of nascent polypeptides to the mitochondrial
571 surface. Biochim. Biophys. Acta 1592, 35-39.

572 Bendtsen, J.D., Nielsen, H., von Heijne, G., Brunak, S., 2004. Improved prediction of
573 signal peptides: SignalP 3.0. J. Mol. Biol. 340, 783-795.

574 Chacinska, A., Koehler, C.M., Milenkovic, D., Lithgow, T., Pfanner, N., 2009.
575 Importing mitochondrial proteins: machineries and mechanisms.Cell 138, 628-644.

576 Ciuffreda, P., Rubino, L., Russo, M., 1998. Molecular cloning and complete nucleotide
577 sequence of galinsoga mosaic virus genomic RNA. Arch. Virol. 143, 173-180.

578 Combet, C., Blanchet, C., Geourjon, C., Deléage, G., 2000. NPS@: network protein
579 sequence analysis. Trends Biochem Sci. 25, 147-150.

580 Cserzö, M., Wallin, E., Simon, I., von Heijne, G., Elofsson, A., 1997. Prediction of
581 transmembrane alpha-helices in prokaryotic membrane proteins: the dense
582 alignment surface method. Prot. Eng. 10, 673-676.

583 Denison, M.R., 2008. Seeking membranes: Positive-strand RNA virus replication
584 complexes. PLoS Biol. 6, e270.

585 Emanuelsson, O., Nielsen, H., Brunak, S., von Heijne, G., 2000. Predicting subcellular
586 localization of proteins based on their N-terminal amino acid sequence. J. Mol.
587 Biol., 300, 1005-1016.
588 Fernández-Miragall, O., Hernández, C., 2011. An internal ribosome entry site directs
589 translation of the 3´-gene from *Pelargonium Flower Break Virus* genomic RNA:
590 implications for infectivity. PLoS One 6, e22617.
591 Galao, R.P., Scheller, N., Alves-Rodrígues, I., Breinig, T., Meyerhans, A., Díez, J.
592 2007. *Saccharomyces cerevisiae*: a versatile eukaryotic system in virology. Microb.
593 Cell Fact. 6, 32.
594 Garavito, R.M., Picot, D., Loll, P.J., 1995. The 3.1 A X-ray crystal structure of the
595 integral membrane enzyme prostaglandin H2 synthase-1. Adv. Prostaglandin
596 Thromboxane Leukot. Res. 23, 99-103.
597 Hua, S., Sun, Z., 2001. Support vector machine approach for protein subcellular
598 localization prediction. Bioinformatics 17, 721-728.
599 Hawkins, J., Bodén, M., 2006. Detecting and sorting targeting peptides with neural
600 networks and support vector machines. J. Bioinform. Comput. Biol. 4, 1-18.
601 Hofmann, K., Stoffel, W., 1993. TMBASE - A database of membrane spanning proteins
602 segments. Biol. Chem. Hoppe-Seyler 374, 166-170.
603 Hwang, Y.T., McCartney, A.W., Gidda, S.K., Mullen, R.T., 2008. Localization of the
604 Carnation Italian ringspot virus replication protein p36 to the mitochondrial outer
605 membrane is mediated by an internal targeting signal and the TOM complex. BMC
606 Cell Biol. 9, 54.
607 Ishibashi, K., Nishikiori, M., Ishikawa, M. 2010. Interactions between tobamovirus
608 replication proteins and cellular factors: their impacts on virus multiplication. Mol.
609 Plant Microbe Interact. 23, 1413-1419.

610 Juretić, D., Zoranić, L., Zucić, D., 2002. Basic charge clusters and predictions of
611 membrane protein topology. J. Chem. Inf. Comput. Sci. 42, 620-632.
612 Ito, H., Fukuda, Y., Murata, K., Kimura, A., 1983. Transformation of intact yeast cells
613 treated with alkali cations. J. Bacteriol. 153, 163-168.
614 Käll, L., Krogh, A., Sonnhammer, E.L., 2007. Advantages of combined transmembrane
615 topology and signal peptide prediction-the Phobius web server. Nucleic Acids Res.
616 35, W429-W432.
617 Kemper, C., Habib, S.J., Engl, G., Heckmeyer, P., Dimmer, K.S., Rapaport, D., 2008.
618 Integration of tail-anchored proteins into the mitochondrial outer membrane does
619 not require any known import components. J. Cell Sci. 121, 1990-1998.
620 Koenig, R., Lesemann, D.E., Pfeilstetter, E., 2009. New isolates of carnation Italian
621 ringspot virus differ from the original one by having replication-associated proteins
622 with a typical tombusvirus-like N-terminus and by inducing peroxisome- rather than
623 mitochondrion-derived multivesicular bodies. Arch. Virol. 154, 1695-1698.
624 Koonin, E.V., 1991. The phylogeny of RNA-dependent RNA polymerases of positive-
625 strand RNA viruses. J. Gen. Virol. 72, 2197-2206.
626 Koonin, E.V., Dolja, V.V., 1993. Evolution and taxonomy of positive-strand RNA
627 viruses: implications of comparative analysis of amino acid sequences. Crit. Rev.
628 Biochem. Mol. Biol. 28, 375-430.
629 Kuo-Chen, Ch., Hong-Bin, S., 2010. A New Method for Predicting the Subcellular
630 Localization of Eukaryotic Proteins with Both Single and Multiple Sites: Euk-
631 mPLoc 2.0. PLoS One 5, e9931.
632 Lesemann, D.E., Adam, G., 1994. Electron microscopical and serological studies on
633 four isometrical pelargonium viruses. Acta Hortic. 377, 41-54.

634 Lomize, M.A., Lomize, A.L., Pogozheva, I.D., Mosberg, H.I., 2006. OPM: Orientations
635 of proteins in membranes database. Bioinformatics 22, 623-625.
636 McCartney, A.W., Greenwood, J.S., Fabian, M.R., White, K.A., Mullen, R.T., 2005.
637 Localization of the tomato bushy stunt virus replication protein p33 reveals a
638 peroxisome-to-endoplasmic reticulum sorting pathway. Plant Cell 17, 3513-3531.
639 Mackenzie, J., 2005. Wrapping things up about virus RNA replication. Traffic 6, 967-
640 977.
641 Martínez-Turiño, S., Hernández, C., 2009. Inhibition of RNA silencing by the coat
642 protein of *Pelargonium flower break virus*: distinctions from closely related
643 suppressors. J. Gen. Virol. 90, 519-525.
644 Martínez-Turiño, S., Hernández, C., 2010. Identification and characterization of RNA
645 binding activity in the ORF1-encoded replicase protein of *Pelargonium flower*
646 *break virus*. J. Gen. Virol. 91, 3075-3084.
647 Martínez-Turiño, S., Hernández, C., 2011. A membrane-associated movement protein
648 of *Pelargonium flower break virus* shows RNA-binding activity and contains a
649 biologically relevant leucine zipper-like motif. Virology 413, 310-319.
650 Miller, D.J., Schwartz, M.D., Ahlquist, P. 2001. Flock house virus RNA replicates on
651 outer mitochondrial membranes in *Drosophila* cells. J. Virol. 75, 11664-11676.
652 Mochizuki, T., Hirai, K., Kanda, A., Ohnishi, J., Ohki, T., Tsuda, S., 2009. Induction of
653 necrosis via mitochondrial targeting of *Melon necrotic spot virus* replication protein
654 p29 by its second transmembrane domain. Virology 390, 239-249.
655 Nagy, P.D., 2008. Yeast as a model host to explore plant virus-host interactions. Annu.
656 Rev. Phytopathol. 46, 217-242.

Nakai, T., Yasuhara, T, Fujiki, Y., Ohashi, A., 1995. Multiple Genes, including a member of the AAA family, are essential for degradation of unassembled subunit 2 of cytochrome c oxidase in yeast mitochondria. Mol. Cell Biol. 15, 4441-4452.

Navarro, B., Rubino, L., Russo, M., 2004. Expression of the *Cymbidium ringspot virus* 33-kilodalton Protein in *Saccharomyces cerevisiae* and molecular dissection of the peroxisomal targeting Signal. J. Virol. 78, 4744-4752.

Orgel, J.P., 2004. Sequence context and modified hydrophobic moment plots help identify 'horizontal' surface helices in transmembrane protein structure prediction. J. Struct. Biol. 148, 51-65.

Orgel, J.P., 2006. Surface-active helices in transmembrane proteins. Curr. Protein Pept. Sci. 7, 553-560.

Panavas, T., Hawkins, C.M., Panaviene, Z., Nagy, P.D., 2005. The role of the p33:p33/p92 interaction domain in RNA replication and intracellular localization of p33 and p92 proteins of *Cucumber necrosis* tombusvirus. Virology 338, 81-95.

Peña, L., Cervera, M., Ghorbel, R., Domínguez, A., Fagoaga, C., Juárez, J., Pina, J.A., Navarro, L., 2003. Transgenic citrus, in: Singh, I.R.P., Jaiwal, P.K. (Eds.), Plant Genetic Engineering, Improvement of Commercial Plants (Volume 3). SCI Tech Publishing LLC, Houston, TX, U.S.A., pages 261-282.

Pogany, J., White, K.A., Nagy, P.D., 2005. Specific binding of tombusvirus replication protein p33 to an internal replication element in the viral RNA is essential for replication. J. Virol. 79, 4859-4869.

Poot, M., Zhang, Y.Z., Krämer, J.A., Wells, K.S., Jones, L.J., Hanzel, D.K. Lugade, A.G., Singer, V.L., Haugland, R.P., 1996. Analysis of mitochondrial morphology and function with novel fixable fluorescent stains. J. Histochem. Cytochem. 44, 1363-1372.

682 Rajendran, K.S., Nagy, P.D., 2003. Characterization of the RNA-binding domains in the
683 replicase proteins of tomato bushy stunt virus. J. Virol. 77, 9244-9258.
684 Rajendran, K.S., Nagy, P.D., 2006. Kinetics and functional studies on interaction
685 between the replicase proteins of *Tomato bushy stunt virus*: requirement of p33:p92
686 interaction for replicase assembly. Virology 345, 270-279.
687 Rico, P., Hernández, C., 2004. Complete nucleotide sequence and genome organization
688 of *Pelargonium flower break virus*. Arch. Virol. 149, 641-651.
689 Rico, P., Hernández, C., 2006. Infectivity of in vitro transcripts from a full-length
690 cDNA clone of *Pelargonium flower break virus* in an experimental and a natural
691 host. J. Plant Path. 88, 103-106.
692 Rose, A., Lorenzen, S., Goede, A., Gruening, B., Hildebrand, P.W., 2009. RHYTHM -
693 a server to predict the orientation of transmembrane helices in channels and
694 membrane-coils. Nucleic Acids Res. 37, W575-W580.
695 Rost B., 1996. PHD: predicting one-dimensional protein structure by profile-based
696 neural networks. Methods Enzymol. 266, 525-539.
697 Rubino, L, Di Franco, A, Russo, M., 2000. Expression of a plant virus non-structural
698 protein in *Saccharomyces cerevisiae* causes membrane proliferation and altered
699 mitochondrial morphology. J. Gen. Virol. 81, 279-286.
700 Rubino, L., Weber-Lotfi, F., Dietrich, A., Stussi-Garaud, C., Russo, M., 2001. The open
701 reading frame 1-encoded ("36K") protein of *Carnation Italian ringspot virus*
702 localizes to mitochondria. J. Gen. Virol. 82, 29-34.
703 Salonen, A., Ahola, T., Kääriäinen, L., 2005. Viral RNA replication in association with
704 cellular membranes. Curr. Top. Microbiol. Immunol. 285, 139-173.

Setoguchi, K., Otera, H., Mihara, K., 2006. Cytosolic factor- and TOM-independent import of C-tail-anchored mitochondrial outer membrane proteins. EMBO J. 25, 5635-5647.

Siggers, K.A., Lesser, C.F., 2008. The yeast *Saccharomyces cerevisiae*: a versatile model system for the identification and characterization of bacterial virulence proteins. Cell Host and Microbe 4, 8-15.

Stork, J., Kovalev, N., Sasvari, Z., Nagy, P.D., 2011. RNA chaperone activity of the tombusviral p33 replication protein facilitates initiation of RNA synthesis by the viral RdRp *in vitro*. Virology 409, 338-347.

Schwer, B., Ren, S., Pietschmann, T., Kartenbeck, J., Kaehlcke, K., Bartenschlager, R., Yen, T.S., Ott, M. 2004. Targeting of hepatitis C virus core protein to mitochondria through a novel C-terminal localization motif. J Virol. 78, 7958-7968.

Turner, K.A., Sit, T.L., Callaway, A.S., Allen, N.S., Lommel, S.A., 2004. Red clover necrotic mosaic virus replication proteins accumulate at the endoplasmic reticulum. Virology 320, 276-290.

Viklund, H., Elofsson, A., 2008. OCTOPUS: improving topology prediction by two-track ANN-based preference scores and an extended topological grammar. Bioinformatics 24, 1662-1668.

Wallis, J.W., Chrebet, G., Brodsky, G., Rolfe, M., Rothstein, R., 1989. A hyper-recombination mutation in *S. cerevisiae* identifies a novel eukaryotic topoisomerase. Cell 58, 409-419.

Weber-Lotfi, F., Dietrich, A., Russo, M., Rubino, L., 2002. Mitochondrial targeting and membrane anchoring of a viral replicase in plant and yeast cells. J. Virol. 76, 10485-10496.

729 Winzeler, E.A., Shoemaker, D.D., Astromoff, A., Liang, H., Anderson, K., Andre, B.,
730 Bangham, R., Benito, R., Boeke, J.D., Bussey, H., Chu, A.M., Connelly, C., Davis,
731 K., Dietrich, F., Dow, S.W., El Bakkoury, M., Foury, F., Friend, S.H., Gentalen, E.,
732 Giaever, G., Hegemann, J.H., Jones, T., Laub, M., Liao, H., Liebundguth, N.,
733 Lockhart, D.J., Lucau-Danila, A., Lussier, M., M'Rabet, N., Menard, P., Mittmann,
734 M., Pai, C., Rebischung, C., Revuelta, J.L., Riles, L., Roberts, C.J., Ross-
735 MacDonald, P., Scherens, B., Snyder, M., Sookhai-Mahadeo, S., Storms, R.K.,
736 Véronneau, S., Voet, M., Volckaert, G., Ward, T.R., Wysocki, R., Yen, G.S., Yu,
737 K., Zimmermann, K., Philippsen, P., Johnston, M., Davis, R.W., 1999. Functional
738 characterization of the S. cerevisiae genome by gene deletion and parallel analysis.
739 Science 285, 901-906.
740 Yu, C.S., Chen, Y.C., Lu, C.H., Hwang, J.K., 2006. Prediction of protein subcellular
741 localization. Proteins 64, 643-651.
742 Yuan, Z., Mattick, J.S., Teasdale, R.D., 2004. SVMtm: support vector machines to
743 predict transmembrane segments. J. Comput. Chem. 25, 632-636.
744 Zinser, E., Paltauf, F., Daum, G., 1993. Sterol Composition of yeast organelle
745 membranes and subcellular distribution of enzymes involved in sterol metabolism.
746 J. Bacteriol. 175, 2853-2858.
747

LEGENDS TO FIGURES

Fig. 1. Intracellular distribution of reporter-tagged viral replicases in yeast cells. Confocal laser scanning microscopy was used for observation of fluorescence in *S. cerevisiae* cells expressing unfused GFP, PFBV p27GFP, PFBV p27GFP plus p86mRFP and CIRV p36GFP. GFP fluorescence is shown in left micrographs, MitoTracker Orange (MT) or mRFP derived fluorescence is shown in middle micrographs, and an overlay of GFP and MT/mRFP signals (Merge) is shown in right micrographs. Untransformed yeast cells labeled with MitoTracker Orange alone, are also included to give an indication of mitochondrial appearance in cells that do not express any viral replicase.

Fig. 2. Confocal laser scanning micrographs of *N. benthamiana* protoplasts expressing unfused GFP or p27GFP. Cells were also stained with MitoTracker Orange (MT) to label the mitochondria, and an overlay of the GFP and MitoTracker signals is included (Merge).

Fig. 3. Western blot analyses of mitochondrial fractions from GFP- and p27GFP-expressing yeast cells. (A) Accumulation of non-fused GFP and p27GFP in the pellets corresponding to mitochondrial enriched-fractions and the accompanying supernatants. (B) Immunoblot analysis of mitochondrial extracts from cells expressing p27GFP either untreated (control) or treated with carbonate, urea, or KCl and then separated by centrifugation into supernatant and pellet fractions.

Fig. 4. Analysis of subcellular localization patterns of p27-deletion derivatives with a C-terminal GFP tag in yeast cells. Amino acid residues of p27 retained in mutants 1 to 7 are indicated. GFP (left micrographs) and Mitotracker Orange (MT; middle micrographs) fluorescence images are shown for the same cells an merged pictures are also provided (right micrographs). Other details as in Fig. 1.

Fig. 5. Analysis of subcellular localization patterns of p27-deletion derivatives with a C-terminal GFP tag in yeast cells. Amino acid residues of p27 retained in mutants 8 to 13 are indicated. GFP (left micrographs) and Mitotracker Orange (MT; middle micrographs) fluorescence images are shown for the same cells and merged pictures are also provided (right micrographs). Other details as in Fig. 1.

Fig. 6. Confocal laser scanning micrographs of *N. benthamiana* protoplasts expressing GFP-tagged deletion mutants of p27. Cells were also stained with MitoTracker Orange (MT) to label the mitochondria, and an overlay of the GFP and MitoTracker signals is included (Merge).

Fig. 7. Subcellular localization patterns of p27 in knockout yeast strains. Construct pYES-p27GFP was transformed in the corresponding yeast mutant (see Table 1 for nomenclature) and GFP fluorescence was monitored through confocal laser scanning microscopy. Cells were also stained with MitoTracker Orange (MT) to label the mitochondria, and an overlay of the GFP and MitoTracker signals is included (Merge).

Fig. 8. (A) Schematic representation of α-helices predicted in p27 sequence. Helix 1 (striped box), corresponding to the only TM region (8-28 aa) obtained from a set of

796 softwares, is located at N-terminus extreme. Other helices (gray boxes) resulting from
797 the use of NPSA, are distributed along the sequence: Helix 2 (39-49), Helix 3 (67-96),
798 Helix 4 (139-152), Helix 5 (162-174), Helix 6 (181-188), Helix 7 (191-215) and Helix 8
799 (222-226). Regions involved in mitochondrial targeting (21-50 and 216-243) are
800 showed on top as black bars. (B) Output plot from HHELIX applied to the predicted
801 helices. Partitioning into surface helical (SM), membrane-spanning (TM) or located in
802 extramembranous domains (EXT) is marked by boundary boxes. μH (Y-axis):
803 hydrophobic moment with aromatic weight. δH (X-axis): average hydrophobicity with
804 aromatic weight added.

Table 1. List of yeast mutants checked for possible alterations in p27 subcellular localization pattern

Gene name [a]	Function	Localization [b]
TOM Complex		
TOM70	Acts as receptor for incoming precursor proteins	OM
TOM7	Promotes assembly and stability of the TOM complex	OM
TOM6	Promotes assembly and stability of the TOM complex	OM
TOM5	Involved in transfer of precursors from the Tom70 and Tom20 receptors to the Tom40 pore	OM
TOM71 (alias TOM72)	Protein translocase 72-kDa with similarity to Tom70	OM
SAM Complex		
SAM37	Binds precursors of β-barrel proteins and facilitates their outer membrane insertion. Contributes to SAM complex stability	OM
TIM Complex		
TIM9	Forms part of a chaperone complex involved in targeting of proteins to specific mitochondrial membranes	ITM
ERMES Complex		
MDM34	Maintains wild-type mitochondrial morphology	OM
MDM10	Subunit of both the ERMES and SAM complex required for normal mitochondrial morphology and inheritance	OM
MMM1	Regulates mitochondrial shape/structure and participates in β-barrel assembly pathway	OM/ERM
NAC complex		
EGD1	Beta subunit of the NAC complex involved in protein targeting	undefined
EGD2	Alpha subunit of the NAC complex involved in protein sorting and translocation	undefined
Ubiquitin-proteasome		
UBX2 (Alias *SEL1*)	Ubiquitin- regulatory protein	OM/ERM
UBP16	Ubiquitin-specific protease	OM
Porins		
POR1	Maintenance of mitochondrial osmotic stability and mitochondrial membrane permeability	OM
POR2	Putative mitochondrial porin	OM
Others		
MSP1	Putative membrane-spanning ATPase involved in intramitochondrial sorting of proteins	OM
MIR1	Mitochondrial phosphate carrier	IM
GEM1	GTPase which regulates mitochondrial morphology	OM
UGO1	Component of the mitochondrial fusion machinery	OM
OM45	Major constituent of the mitochondrial outer membrane with unknown function	OM
MMR1	Phosphorylated protein that mediates mitochondrial distribution to buds	OM

[a] TOM, translocase of outer membrane; SAM, sorting and assembly machinery; TIM, translocase of the inner mitochondrial membrane; ERMES complex, ER-mitochondria encounter structure; NAC, nascent polypeptide-associated complex.

[b] OM, outer membrane; IM, inner membrane; ITM, intermembrane space; ERM, endoplasmic reticulum membrane.

Figure 1

Click here to download high resolution image

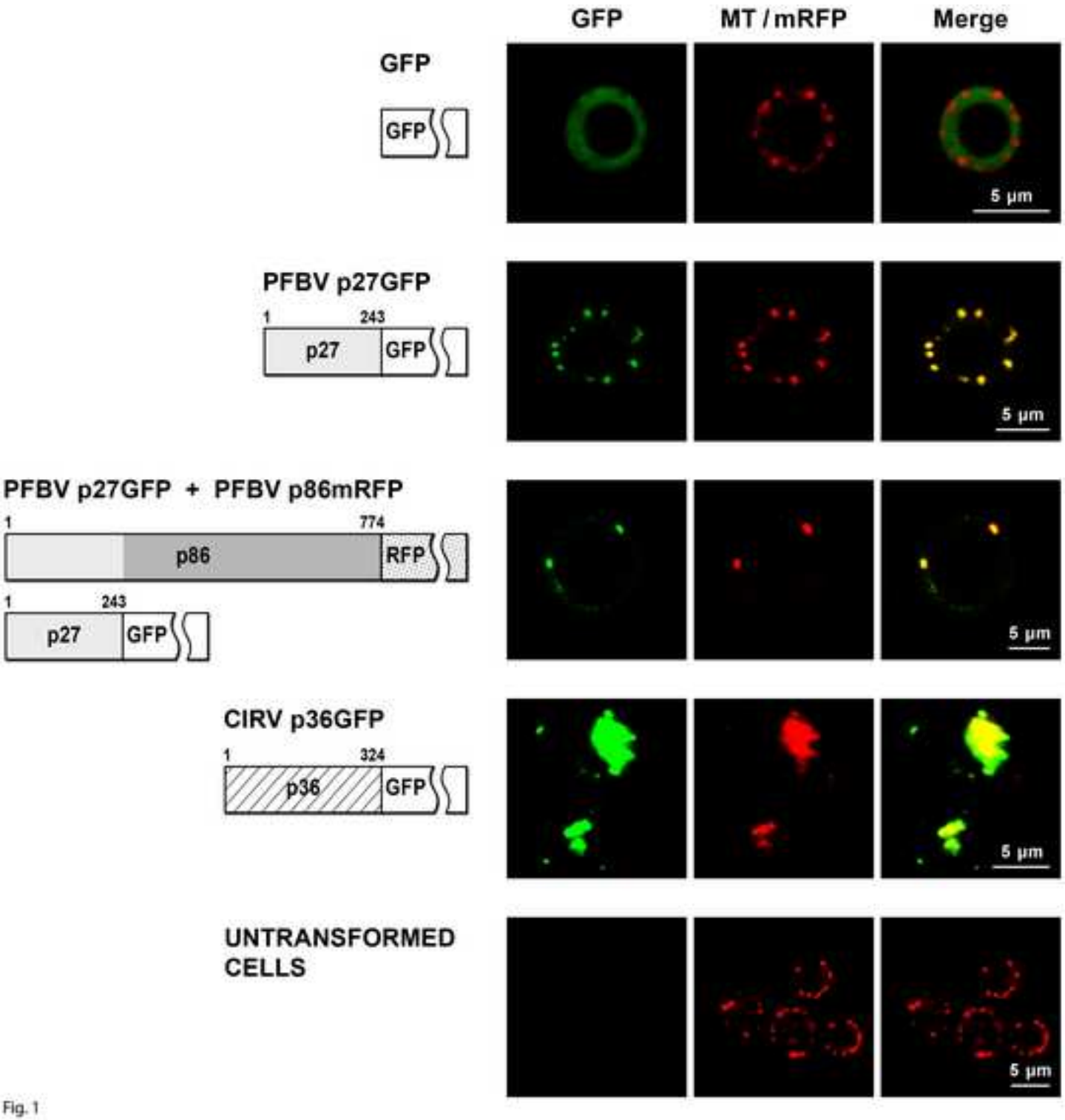

Fig. 1

Figure 2
Click here to download high resolution image

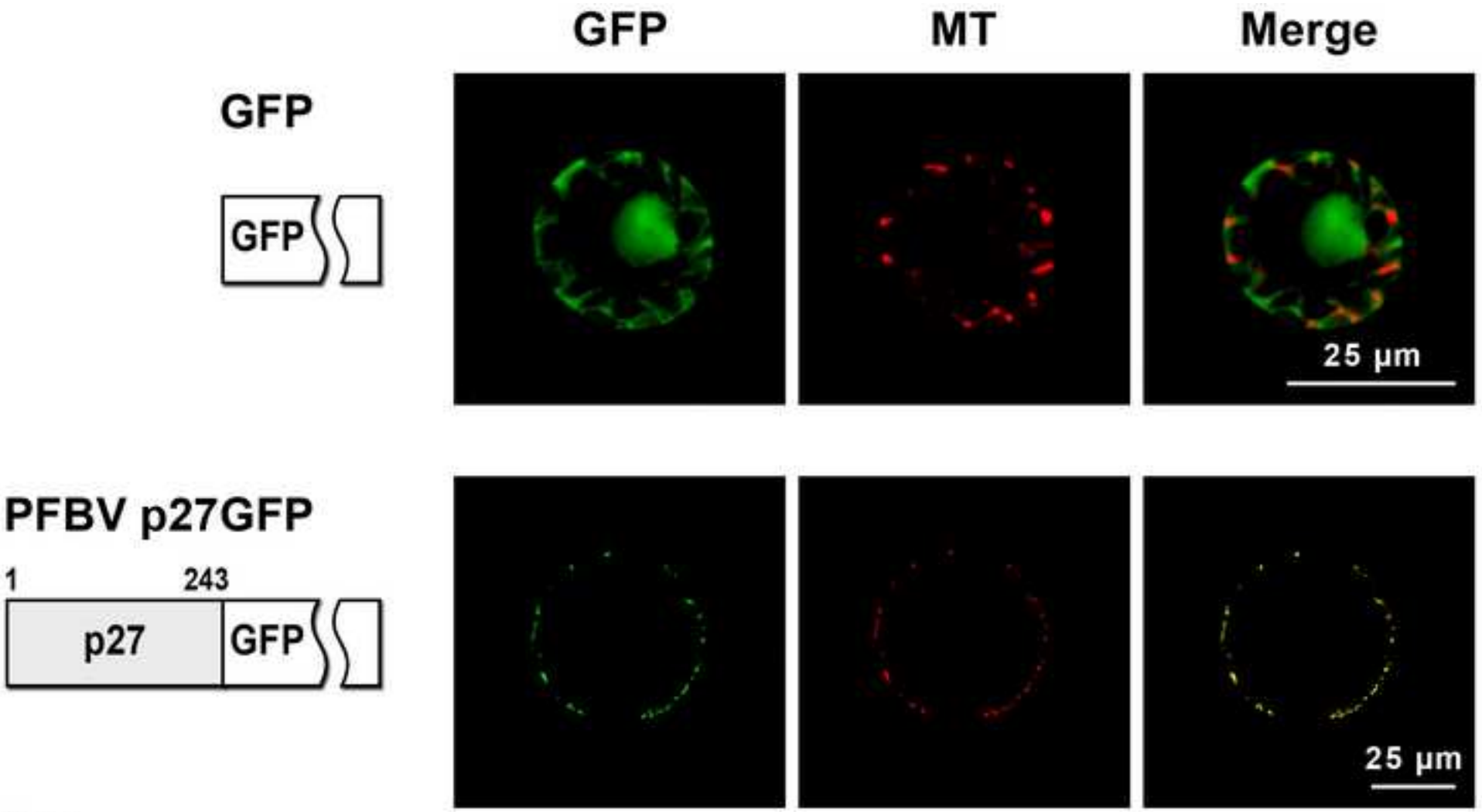

Fig. 2

Figure 3

Click here to download high resolution image

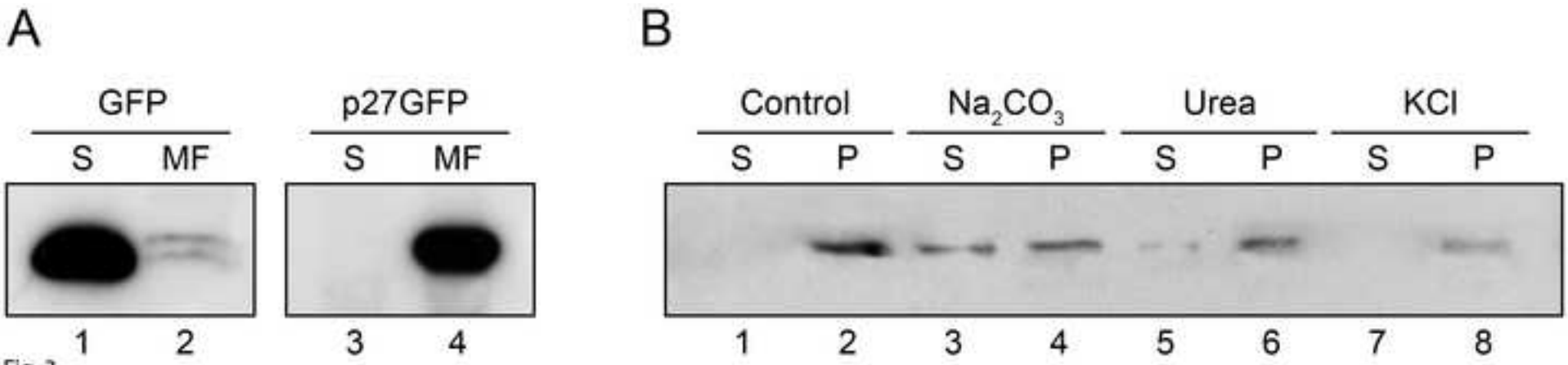

Fig. 3

Figure 4

Click here to download high resolution image

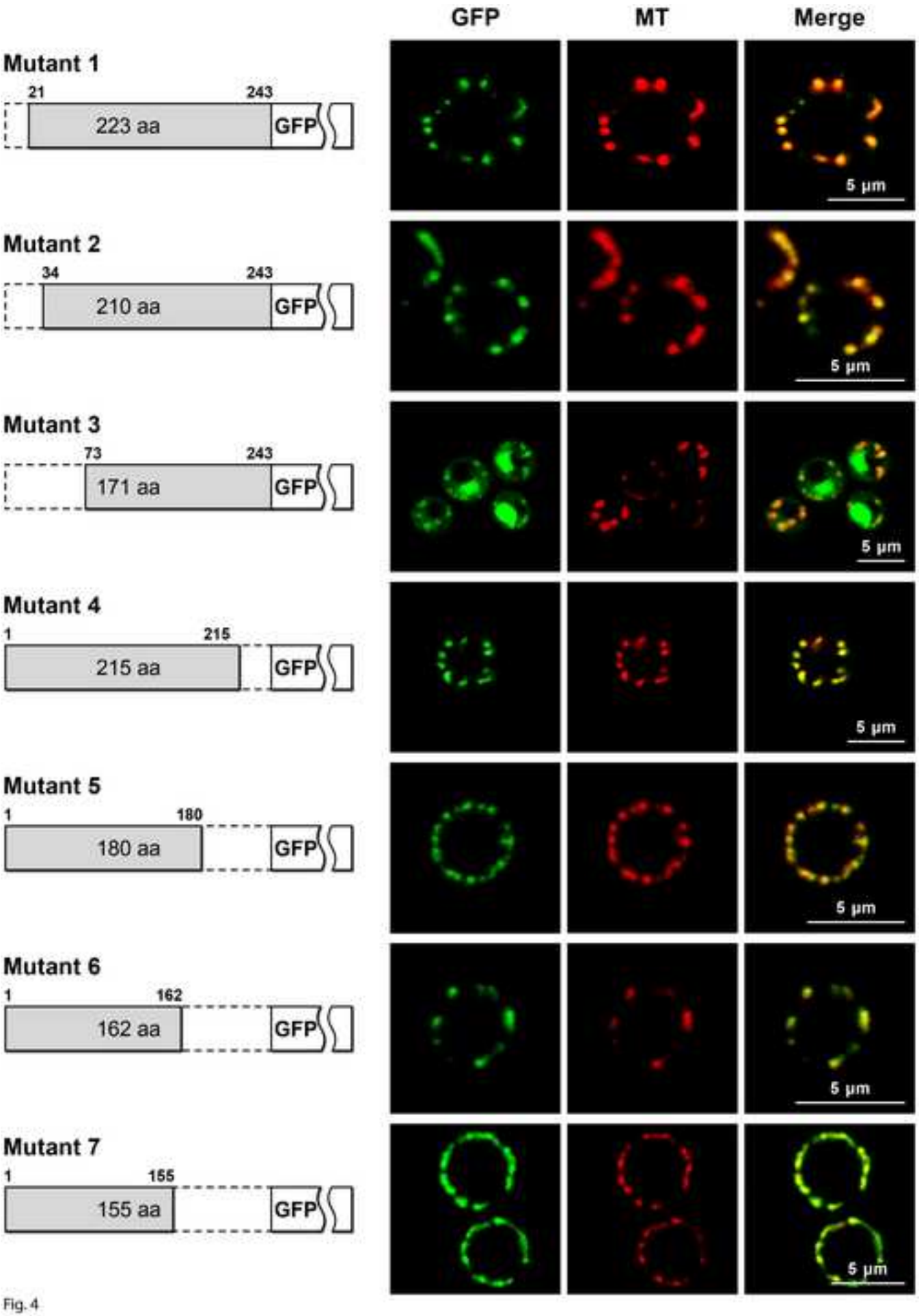

Fig. 4

Figure 5

Click here to download high resolution image

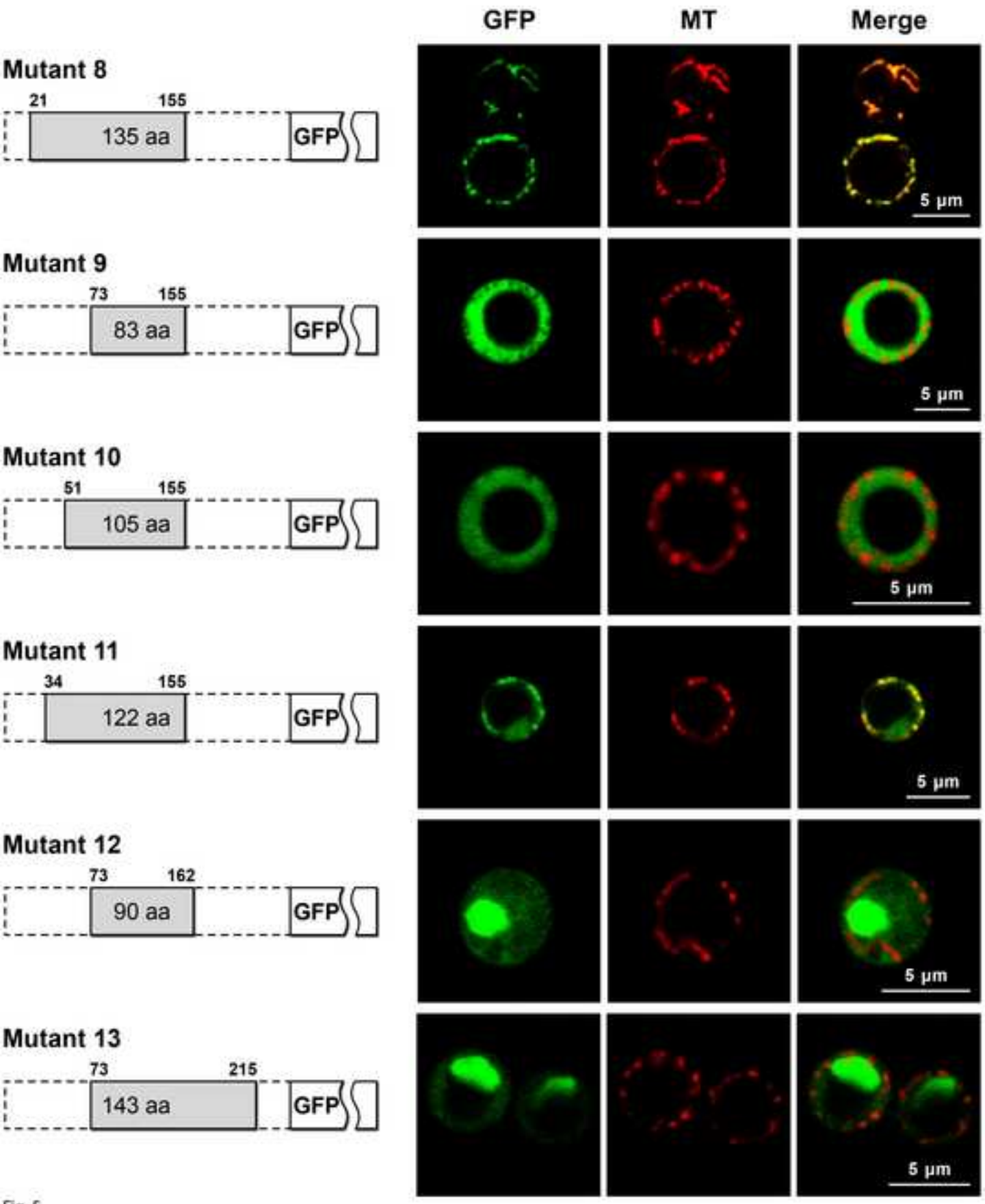

Fig. 5

Figure 6

Click here to download high resolution image

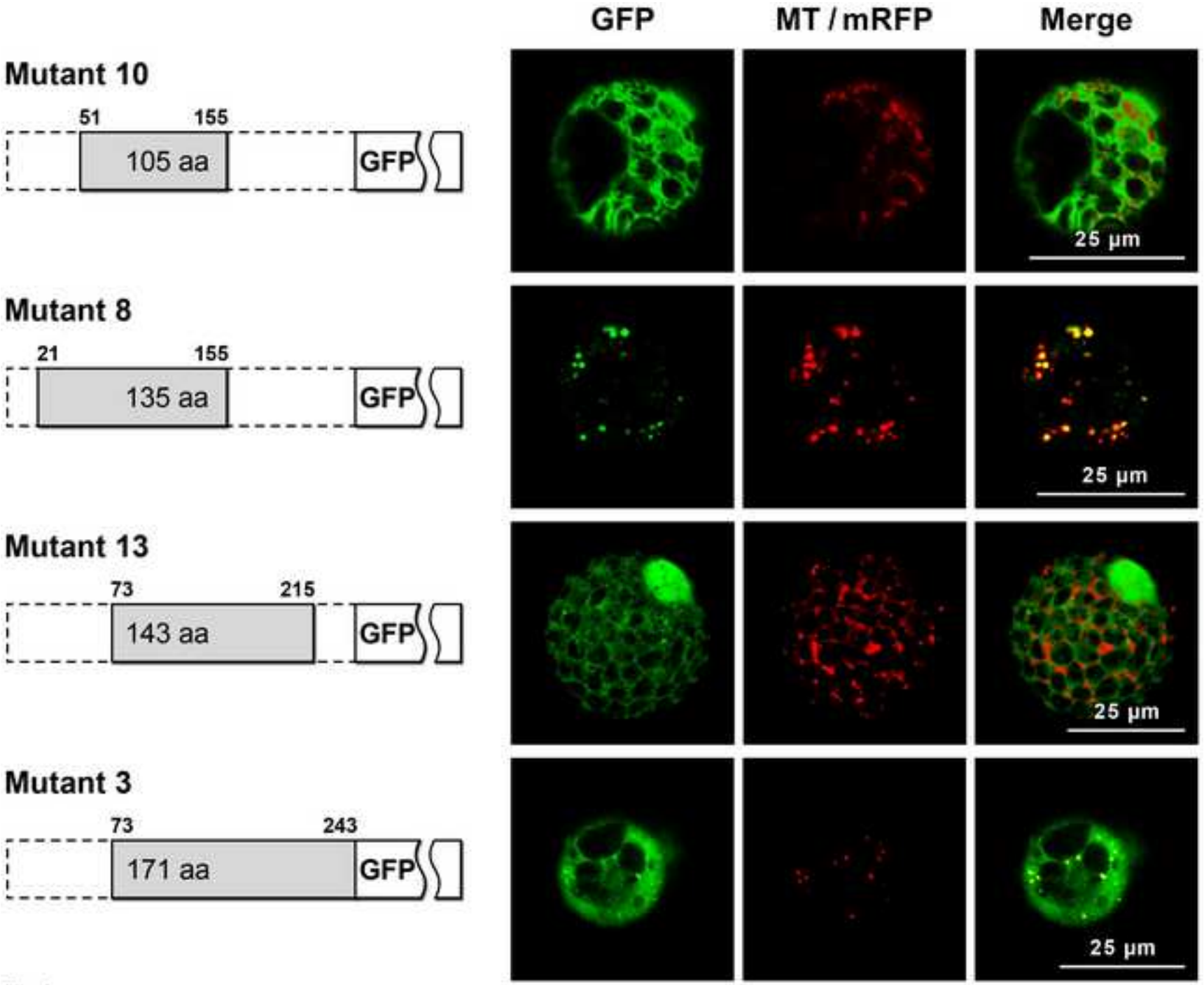

Fig. 6

Figure 7

Click here to download high resolution image

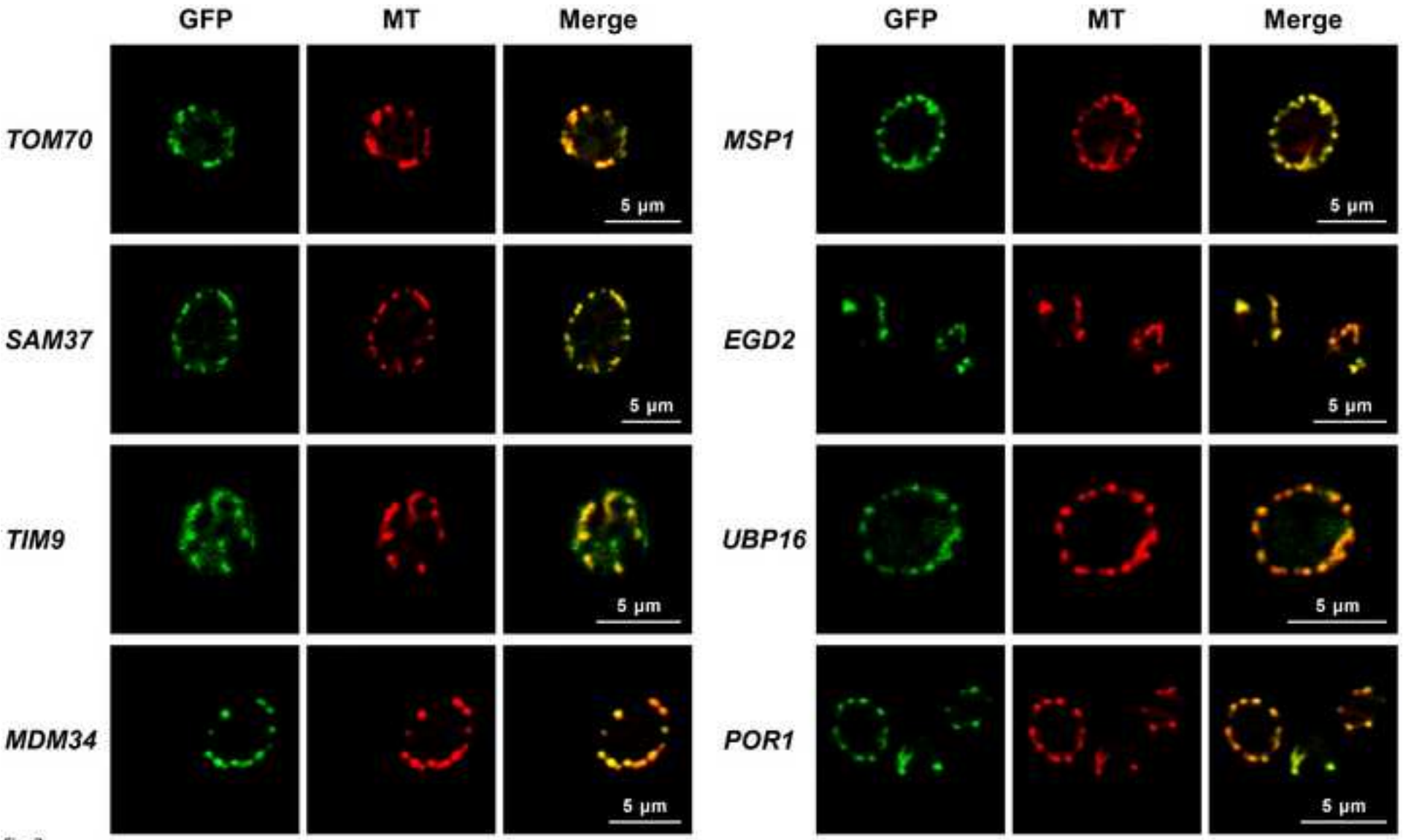

Fig. 7

Figure 8

Click here to download high resolution image

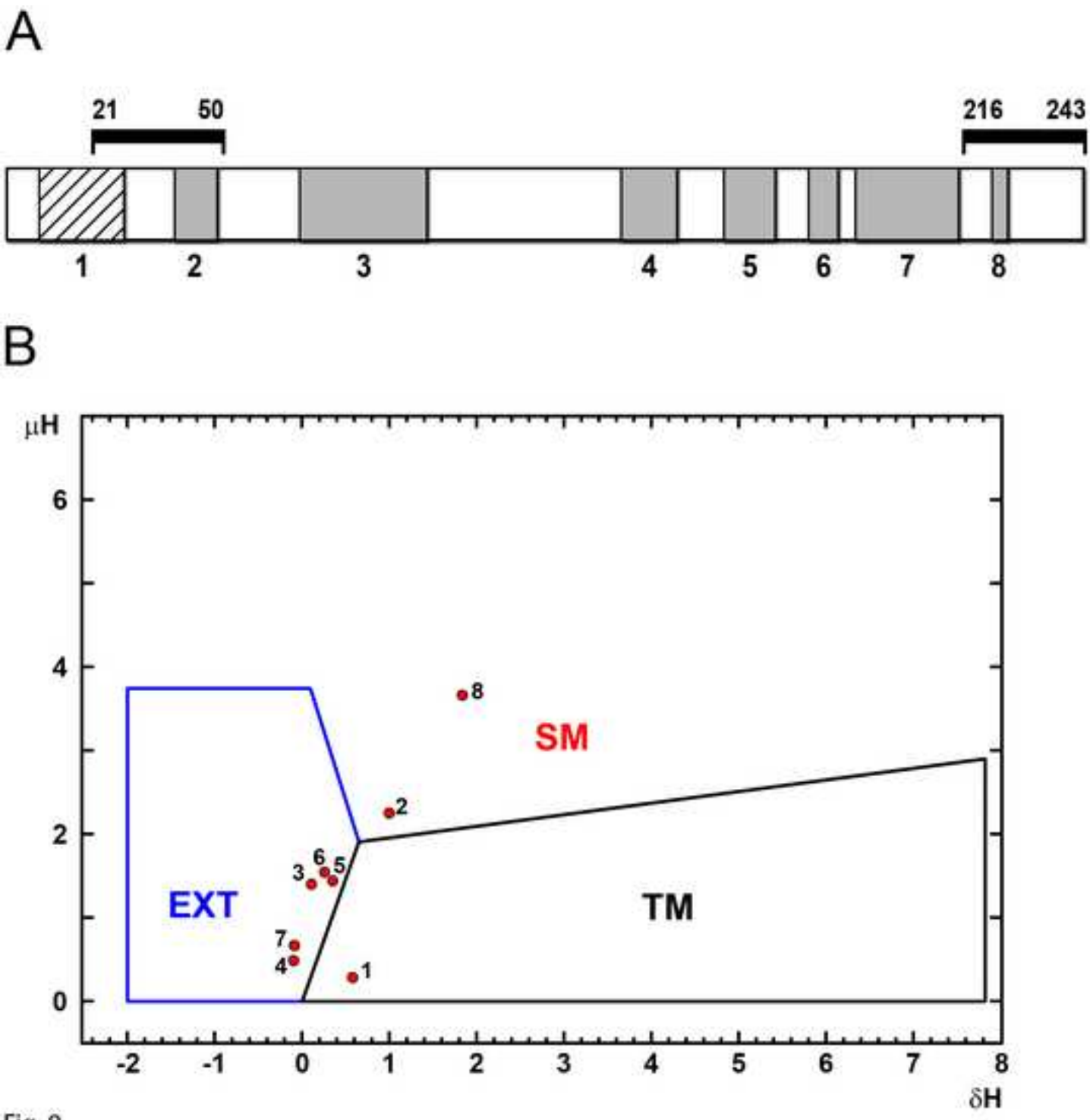

Fig. 8

Supplementary TableS1

Click here to download Supplementary Material: SupplemenTableS1.doc